Electronic Supplementary Material (ESI) for Physical Chemistry Chemical Physics.

Supporting Information

Solvent Effects on Ion-Receptor Interactions in the Presence of an External Electric Field

Martin Novak[1], Cina Foroutan-Nejad[1]*, Radek Marek[1,2],

[1] CEITEC – Central European Institute of Technology, Masaryk University, Kamenice 5/A4, CZ-625 00, Brno, Czech Republic

[2] Department of Chemistry, Faculty of Science, Masaryk University, Kamenice 5/A4, CZ-625 00 Brno, Czech Republic

Corresponding Author e-mail: cina.foroutannejad@ceitec.muni.cz

On the Mechanism of Electron-Transfer between Ion and π-receptor

In the present work we briefly considered bonding mechanism and possible mechanism for charge-transfer between the ions and receptors. Because the observed mechanism is more or less comparable with gas-phase mechanism[1] and the solvent effect follows a predictable pattern, we do not discuss this issue in the main text.

It is known that an EEF not only affects the energy of the ground-state of the system, but it influences also the excited states;[2,3] in particular, the excited-state(s), corresponding to the electron-transfer between the ion and the receptor, (here after abbreviated **CTES**).[1] As the energy of a **CTES** decreases it approaches the ground-state. Recently we have demonstrated that decreasing energy of the **CTES** increases the binding energy[1] via increasing the multi-center electron-sharing[4] that follows charge-shift mechanism of covalency.**Error! Bookmark not defined.**[5] Here, we emphasize that the same phenomenon is responsible for an increase in the probability of faradaic electron transfer between the receptor and the ions. Employing the resonance structures operative in the process within the context of the valence bond theory (**VBT**) helps to demonstrate this idea, **Equations 2** and **3**.

$$\Psi_{X^-\ldots Rec} = \varphi_{X\uparrow\downarrow^-\ldots Rec} + \varphi_{X\uparrow\cdots[\downarrow Rec]^-} + \varphi_{[X\uparrow\downarrow Rec]^-} \qquad \textbf{Equation 2}$$

$$\Psi_{Y^+\ldots Rec} = \varphi_{Y^+\ldots\uparrow\downarrow Rec} + \varphi_{Y\uparrow\cdots[\downarrow Rec]^+} + \varphi_{[Y\uparrow\downarrow Rec]^+} \qquad \textbf{Equation 3}$$

The first term in the RHS of **Equations 2** and **3** corresponds to the ground-states of the anionic/cationic complexes, the second term represents the wave function of a **CTES** and the third denotes an insignificant contribution from a covalence-type resonance structure. It is clear from **Equations 2** and **3** that the same factor that increases the state-mixing, i.e. the proximity of

energy levels of the first and the second terms, increases the probability of faradaic electron-transfer via involving the electron sharing and the contribution from the third term. Computing the excited-state energies for the model systems reveals a considerable energy change for the **CTES**(s); this is in particular more evident for the softer species, **Figure S1**.

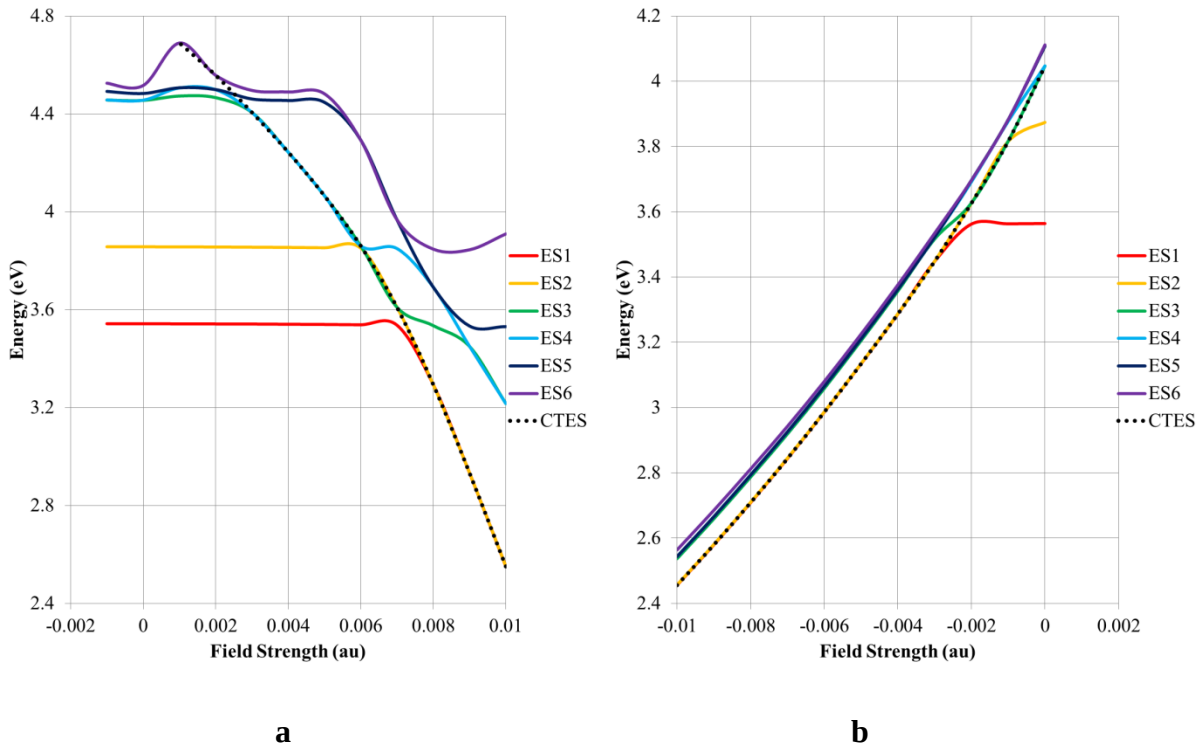

Figure S1. Schematic presentation of the energy of first six singlet excited-state with respect to the ground-state versus the EEF for (a) potassium and (b) bromide complexes. The lowest-energy CTES is marked with dotted line; this state is not the lowest-energy singlet-excited-state in the absence of the EEF but the EEF lowers the energy of CTES dramatically, thus in the limit of EEF = 0.01 au, the lowest-energy CTES is the lowest energy singlet-excited-state in most of studied systems (except for fluoride). The plots for the rest of systems are presented in Supporting Information.

To gain an understanding of the nature of the intermediates involved in the electron-transfer process, we employed the QTAIM analysis. The delocalization index, **DI**,[6,7,8,9] defined within the context of the QTAIM, is a measure of the number of electrons shared[10] between two molecular or supramolecular subspaces.[11,12,13] Alternatively, the delocalization index can be interpreted as

the fluctuation of the electronic population of a molecular subspace.[88] A higher **DI** means a *higher probability* of finding an electron in either of the interacting fragments. Therefore, the **DI** between two interacting systems should indicate the role of covalent contribution in the bonding and, by extension. **DI** also portrays the *probability of faradaic electron-transfer* between two interacting systems via Harpoon mechanism[14] that is operative in systems where an intersystem crossing facilitates electron transfer. The **DI** between two interacting systems in the presence of an EEF must increase by increasing the EEF in the direction that promotes electron-transfer. The **DI** value must ideally reach to unity, the maximum value, when the probability of finding electron on either of interacting fragments is equal and then decrease when the electron-transfer is completed. However, in principle tunneling may decrease the maximum magnitude of the **DI** because the electron-transfer process can occur in a near-degeneracy state as well.

As expected from our hypothesis, plotting the **DI** between the ions and the π-system versus the EEF strength reveals the increase in the electron sharing by increasing the electric field in the favorable direction for both the cationic and the anionic systems, **Figure S2**. The magnitude of the **DI** between the ions and the receptor depends on the chemical softness of both fragments; increasing the number of electrons in an ion or the size of carbonic cluster, as has been proven before,[15] increases the **DI**. This is once more consistent with chemist's expectation that the ease of faradaic electron-transfer *in the presence of an EEF* is proportional to the softness/hardness of ions.

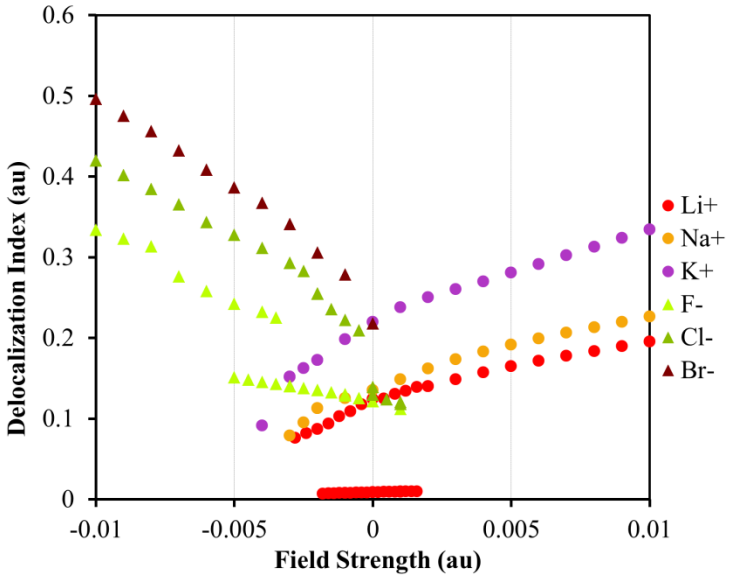

Figure S2. The plot of delocalization index versus strength of EEF; a higher DI reflects a higher probability in faradaic electron-transfer in the binding energy.

Interestingly, while the covalent-type interaction enhances by elevating the EEF strength in favorable direction, the atomic charges change negligibly in the studied range of the EEF. This suggests that faradaic electron-transfer does not occur between the ions and the receptor within ±0.01 au field, **Table S1**. It is worth noting that it has been demonstrated that atomic charges are incapable of tracing charge-transfer via Harpoon mechanism.[14]

The magnitude of the atomic charge variation is somewhat greater for softer ions compared to their harder counterparts as previously was observed in case of modeling the interaction of ions with a Cu surface in the presence of an electric field.[16] The observed variation in the **DI** and negligible electron transfer between the ions and the π-system suggest that the bonding mechanism of ion-receptor complexes changes from a non-covalent to a charge-shift covalent-type as the EEF strength increases. This bonding mechanism is different from the gas-phase bonding mechanism in which ions, in particular anions, form strong covalent-type complexes with π-receptors even in the absence of an EEF.[1,4]

Table S1.Atomic charges obtained from QTAIM computations.

Field	Li^+	Na^+	K^+	Field	F^-	Cl^-	Br^-
0.0100	**0.926**	**0.929**	**0.918**	**-0.0100**	**-0.972**	**-0.929**	**-0.897**
0.0090	**0.928**	**0.931**	**0.922**	**-0.0090**	**-0.975**	**-0.934**	**-0.903**
0.0080	**0.930**	**0.933**	**0.925**	**-0.0080**	**-0.977**	**-0.938**	**-0.910**
0.0070	**0.933**	**0.935**	**0.928**	**-0.0070**	**-0.979**	**-0.943**	**-0.916**
0.0060	**0.935**	**0.938**	**0.931**	**-0.0060**	**-0.983**	**-0.948**	**-0.923**
0.0050	**0.938**	**0.940**	**0.935**	**-0.0050**	**-0.985**	**-0.952**	**-0.928**
0.0040	**0.940**	**0.943**	**0.938**	**-0.0040**	**-0.987**	**-0.955**	**-0.934**
0.0030	**0.943**	**0.946**	**0.941**	**-0.0030**	**-0.988**	**-0.959**	**-0.940**
0.0020	**0.947**	**0.949**	**0.944**	**-0.0020**	**-0.989**	**-0.965**	**-0.947**
0.0010	**0.996**	**0.953**	**0.947**	**-0.0010**	**-0.991**	**-0.972**	**-0.952**
0.0000	**0.997**	**0.958**	**0.951**	**0.0000**	**-0.992**	**-0.981**	**-0.962**
-0.0010	**0.997**	**0.961**	**0.957**	**0.0010**	**-0.993**	**-0.983**	——
-0.0020	——	**0.965**	**0.963**	**0.0020**	——	——	——
-0.0030	——	**0.978**	**0.968**	**0.0030**	——	——	——
-0.0040	——	——	**0.981**	**0.0040**	——	——	——

In summary, the bonding mechanism is an indicator of the redox process mechanism; the electron-transfer occurs via formation of a charge-shift covalent-type ion-receptor complex prior to the faradaic electron-transfer between two fragments in very strong fields.

Supplementary Tables

Tables S2-7. Ion-coronene complex optimized via PCM solvent model. Ion-coronene distance (R_M-Cor) in Å, and binding energy (BE) in kcal/mol are listed below for Li^+, Na^+, K^+, F^-, Cl^-, and Br^- respectively.

Table S2

Field	R_Li-Cor	BE
0.01	2.337	-8.49
0.009	2.355	-7.96
0.008	2.371	-7.49
0.007	2.387	-7.03
0.006	2.400	-6.61
0.005	2.415	-6.2
0.004	2.436	-5.76
0.003	3.108	-0.91
0.002	3.124	-0.82
0.001	3.147	-0.72
0	3.183	-0.76
-0.001	3.225	-0.51

Table S3

Field	R_Na-Cor	BE
0.01	2.362	-7.1
0.009	2.424	-6.88
0.008	2.537	-6.33
0.007	2.569	-5.95
0.006	2.599	-5.57
0.005	2.627	-5.21
0.004	2.669	-4.79
0.003	2.972	-2.93
0.002	3.010	-2.59
0.001	3.425	-0.85
0	3.463	-0.88
-0.001	3.511	-0.62

Table S4

Field	R_K-Cor	BE
0.01	2.668	-7.3
0.009	2.688	-7.06
0.008	2.712	-6.8
0.007	2.749	-6.52
0.006	2.821	-6.23
0.005	2.863	-5.93
0.004	2.890	-5.63
0.003	2.911	-5.33
0.002	2.930	-5.03
0.001	2.953	-4.71
0	3.275	-3.15

Table S5

Field	R_F-Cor	BE
-0.01	2.223	-5.2
-0.009	2.291	-4.98
-0.008	2.351	-4.75
-0.007	2.407	-4.49
-0.006	2.460	-4.21
-0.005	2.509	-3.91
-0.004	2.562	-3.58
-0.003	2.629	-3.2
-0.002	3.561	-0.58
-0.001	3.605	-0.51
0	3.664	-0.56

Table S6

Field	R_Cl-Cor	BE
-0.01	2.721	-3.52
-0.009	2.765	-3.37
-0.008	2.814	-3.22
-0.007	2.872	-3.12
-0.006	3.010	-3.3
-0.005	3.076	-3.16
-0.004	3.131	-2.97
-0.003	3.181	-2.77
-0.002	3.235	-2.56
-0.001	3.603	-1.97
0	3.963	-1.41
0.001	4.051	-1.01
0.002	4.187	-0.77

Table S7

Field	R_Cl-Cor	BE
-0.01	2.866	-3.66
-0.009	2.920	-3.56
-0.008	3.003	-3.59
-0.007	3.073	-3.53
-0.006	3.130	-3.41
-0.005	3.188	-3.27
-0.004	3.240	-3.1
-0.003	3.290	-2.91
-0.002	3.341	-2.72
-0.001	3.680	-2.28
0	3.755	-2.21
0.001	4.159	-1.2
0.002	4.238	-1.04

Table S8. Lithium cation-coronene complex in CCl_4 modeled via PCM. Ion-coronene distance (R_M-Cor) in Å, and binding energy (BE) in kcal/mol are listed below.

Field	R_Li-Cor	BE
0.01	1.922	-36.72
0.009	1.934	-35.79
0.008	1.941	-34.86
0.007	1.950	-33.94
0.006	1.958	-33.03
0.005	1.965	-32.12
0.004	1.973	-31.2
0.003	1.981	-30.29
0.002	1.989	-29.37
0.001	1.999	-28.43
0	2.013	-27.46
-0.001	2.032	-26.41
-0.002	2.060	-25.25
-0.003	2.098	-23.97
-0.004	2.129	-22.78
-0.005	2.423	-17.84
-0.006	2.454	-16.65

Table S9. Lithium cation-coronene complex in hexane modeled via PCM. Ion-coronene distance (R_M-Cor) in Å, and binding energy (BE) in kcal/mol are listed below.

Field	R_Li-Cor	BE
0.01	1.873	-40.19
0.009	1.896	-39.19
0.008	1.909	-38.23
0.007	1.921	-37.27
0.006	1.931	-36.32
0.005	1.940	-35.37
0.004	1.949	-34.42
0.003	1.958	-33.47
0.002	1.968	-32.51
0.001	1.976	-31.55
0	1.987	-30.57
-0.001	1.998	-29.58
-0.002	2.015	-28.49
-0.003	2.044	-27.28
-0.004	2.122	-25.4
-0.005	2.339	-21.42
-0.006	2.361	-20.29

Table S10. Lithium cation-coronene complex in water modeled via PCM and old default cavity model from G03. Ion-coronene distance (R_M-Cor) in Å, and binding energy (BE) in kcal/mol are listed below.

Field	R_Li-Cor	BE
0.01	2.337	-9.29
0.009	2.355	-8.83
0.008	2.371	-8.4
0.007	2.387	-7.95
0.006	2.400	-7.45
0.005	2.415	-7.03
0.004	2.436	-6.58
0.003	3.108	-2.42
0.002	3.124	-2.21
0.001	3.147	-1.97
0	3.183	-1.69
-0.001	3.225	-1.44

Table S11. Lithium cation-coronene complex in water modeled via SMD and old default cavity model from G03. Geometries are taken from old cavity model of PCM. Ion-coronene distance (R_M-Cor) in Å, and binding energy (BE) in kcal/mol are listed below.

Field	R_Li-Cor	BE
0.01	2.337	-18.33
0.009	2.355	-17.64
0.008	2.371	-16.99
0.007	2.387	-16.36
0.006	2.400	-15.75
0.005	2.415	-15.15
0.004	2.436	-14.48
0.003	3.108	-6.95
0.002	3.124	-6.69
0.001	3.147	-6.4
0	3.183	-6.05
-0.001	3.225	-5.71

Attention:

Geometries of all optimized systems are available in xyz format in a zip file via the webpage of publisher.

References

1. M. Novak, C. Foroutan-Nejad, R. Marek, *J. Chem. Theory Comput.*, 2016, **12**, 3788-3795.
2 A. Saenz, *Phys. Rev. A*, 2000, **61**, 051402.
3 A. Saenz, *Phys. Rev. A*, 2002, **66**, 063407.
4 C. Foroutan-Nejad, Z. Badri, R. Marek, *Phys. Chem. Chem. Phys.* 2015, **17**, 30670-30679.
5. S. Shaik, D. Danovich, W. Wu, P. C. Hiberty, *Nature Chem.*, 2009, **1**, 443-449.
6. R. F. W. Bader, M. E. Stephens, *J. Am. Chem. Soc.*, 1975, **97**, 7391-7399.
7. F. Cortés-Guzmán, R. F. W. Bader, *Coord. Chem. Rev.*, 2005, **249**, 633-662.
8. M. García-Revilla, P. L. A. Popelier, E. Francisco, A. Martín-Pendás, *J. Chem. Theory Comput.*, 2011, **7**, 1704-1711.
9. C. Foroutan-Nejad, S. Shahbazian, R. Marek, *Chem. Eur. J.*, 2014, **20**, 10140-10152.
10. M. García-Revilla, E. Francisco, P. L. A. Popelier A. Martín Pendás, *ChemPhysChem*, 2013, **14**, 1211-1218.
11. M. Rafat, P. L. A. Popelier, *The quantum theory of atoms in molecules: from solid state to DNA and drug design* (Eds.: C. F. Matta and R. J. Boyed), Wiley-VCH, Weinheim, 2007, 121-140.
12. Z. Badri, C. Foroutan-Nejad, *Phys. Chem. Chem. Phys.*, 2016, **18**, 11693-11699.
13. Z. Badri, C. Foroutan-Nejad, J. Kozelka, R. Marek, *Phys. Chem. Chem. Phys.*, 2015, **17**, 26183-26190.
14. M. Rodríguez-Mayorga, E. Ramos-Cordoba, P. Salvador, M. Solà, E. Matito, *Mol. Phys.*, 2016, **114**, 1345-1355.
15. C. Foroutan-Nejad, R. Marek, *Phys. Chem. Chem. Phys.*, 2014, **16**, 2508-2514.
16. M. Saracino, P. Broekmann, K. Gentz, M. Becker, H. Keller, F. Janetzko, T. Bredow, K. Wandelt, H. Dosch, *Phys. Rev. B*, 2009, **79**, 115448.